Geosci. Model Dev. Discuss., 8, 715–759, 2015
www.geosci-model-dev-discuss.net/8/715/2015/
doi:10.5194/gmdd-8-715-2015

Geoscientific Model Development Discussions
Open Access

An improved representation of physical permafrost dynamics in the JULES land surface model

S. Chadburn[1], E. Burke[2], R. Essery[3], J. Boike[4], M. Langer[4,5], M. Heikenfeld[4,6], P. Cox[1], and P. Friedlingstein[1]

[1]Earth System Sciences, Laver Building, University of Exeter, North Park Road, Exeter EX4 4QE, UK
[2]Met Office Hadley Centre, Fitzroy Road, Exeter EX1 3PB, UK
[3]Grant Institute, The King's Buildings, James Hutton Road, Edinburgh EH9 3FE, UK
[4]Alfred Wegener Institute, Helmholtz Center for Polar and Marine Research (AWI), 14473 Potsdam, Germany
[5]Laboratoire de Glaciologie et Géophysique de l'Environnement (LGGE) BP 96 38402 St Martin d'Hères CEDEX, France
[6]Atmospheric, Oceanic and Planetary Physics, Department of Physics, University of Oxford, Parks Road, Oxford OX1 3PU, UK

Received: 19 December 2014 – Accepted: 13 January 2015 – Published: 30 January 2015

Correspondence to: S. Chadburn (s.e.chadburn@exeter.ac.uk)

Published by Copernicus Publications on behalf of the European Geosciences Union.

Abstract

It is important to correctly simulate permafrost in global climate models, since the stored carbon represents the source of a potentially important climate feedback. This carbon feedback depends on the physical state of the permafrost. We have therefore included improved physical permafrost processes in JULES, which is the land-surface scheme used in the Hadley Centre climate models.

The thermal and hydraulic properties of the soil were modified to account for the presence of organic matter, and the insulating effects of a surface layer of moss were added, allowing for fractional moss cover. We also simulate a higher-resolution soil column and deeper soil, and include an additional thermal column at the base of the soil to represent bedrock. In addition, the snow scheme was improved to allow it to run with arbitrarily thin layers.

Point-site simulations at Samoylov Island, Siberia, show that the model is now able to simulate soil temperatures and thaw depth much closer to the observations. The root mean square error for the near-surface soil temperatures reduces by approximately 30 %, and the active layer thickness is reduced from being over 1 m too deep to within 0.1 m of the observed active layer thickness. All of the model improvements contribute to improving the simulations, with organic matter having the single greatest impact. A new method is used to estimate active layer depth more accurately using the fraction of unfrozen water.

Soil hydrology and snow are investigated further by holding the soil moisture fixed and adjusting the parameters to make the soil moisture and snow density match better with observations. The root mean square error in near-surface soil temperatures is reduced by a further 20 % as a result.

1 Introduction

The northern high latitudes (NHLs) are an important region in terms of the changing global climate. Both observations and future projections of warming are amplified in this region (Overland et al., 2004; Bekryaev et al., 2010; Stocker et al., 2013). At the land-surface scale, significant thawing of permafrost has already been observed in many areas (Camill, 2005; Romanovsky et al., 2010, 2013).

Permafrost stores large quantities of carbon (Tarnocai et al., 2009), and this could be released in the form of carbon dioxide and methane as the permafrost thaws, causing a positive feedback effect on the climate (Khvorostyanov et al., 2008; Koven et al., 2011; Schaphoff et al., 2013; Burke et al., 2012; Schneider von Deimling et al., 2012). It is therefore important to simulate NHLs realistically in global climate models (GCMs) and land surface models, which are used to make future climate projections and inform emissions targets (Stocker et al., 2013).

In order to include permafrost carbon feedbacks in land surface models, the first requirement is that the physics is simulated correctly. This includes thaw depth and rate of thaw, hydrological processes and soil temperature dynamics, which all affect soil carbon stocks and decomposition rate (Gouttevin et al., 2012b; Exbrayat et al., 2013).

While permafrost-specific models have made progress towards correctly simulating permafrost dynamics (Riseborough et al., 2008; Jafarov et al., 2012; Westermann et al., 2014), in global land-surface models the Arctic has often been neglected, leading to the large discrepancies between models and reality seen in Koven et al. (2012). One reason that the NHLs are poorly represented in global models is the difficulty of obtaining observations with which to drive and evaluate the models. Harsh conditions in the Arctic mean that much of the land area is difficult to access, and detailed simulations are only possible on small scales. However, the use of small-scale simulations where observations are available can help to improve the large-scale dynamics. Several global land-surface models have already improved their representation of permafrost physics

GMDD
8, 715–759, 2015

(Beringer et al., 2001; Lawrence and Slater, 2008; Gouttevin et al., 2012a; Ekici et al., 2014a).

In this paper we add new permafrost-relevant processes into JULES (Joint UK Land Environment Simulator), which is the land-surface scheme in the Hadley Centre climate models and will be used in the first UK Earth System Model (Best et al., 2011; Clark et al., 2011), improving on the past implementation of these processes (Christensen and Cox, 1995; Cox et al., 1999). We evaluate the model at a site level, where it is reasonable to compare the model directly with observational data and a large quantity of data is available. Being able to simulate realistically at a site level shows that the physics of the model is correct, which is a prerequisite for trusting large-scale simulations. These developments are included in large-scale simulations in Chadburn et al. (2015) (in prep).

JULES already includes some of the processes that are important for permafrost: the effects of soil freezing and thawing on the energy budget, and more recently a multilayer snow scheme, which significantly improves model performance (Burke et al., 2013). However, systematic differences between JULES simulations and reality have been identified. When compared with observations of active layer thickness (ALT) (maximum depth of summer thaw), the simulated active layer in JULES is consistently too deep. This is seen, for example, in Dankers et al. (2011), where the simulated active layer was compared with observations from over 100 sites in the CALM active layer monitoring programme (Brown et al., 2000). This bias in ALT indicates that the soil may warm too quickly in summer, which would lead to an amplification of the annual cycle of soil temperatures. This amplification is indeed observed in JULES (Burke et al., 2013). This suggests that the model undergoes an accelerated soil warming in summer, meaning either that too much heat enters the soil or too much of that heat accumulates near the surface.

There are two controls on the amount of heat entering and leaving the soil: that is the land-cover above the soil and the thermal properties of the soil itself. In particular, soil organic matter and the moss layer that is often present in the low Arctic can greatly influence the ALT and summer soil temperatures (Dyrness, 1982). This is because moss and organic matter have insulating properties, and can also hold more water than mineral soils. The importance of accounting for organic matter in land-surface models has been discussed in e.g. Rinke et al. (2008); Lawrence et al. (2008); Koven et al. (2009). Snow also insulates the soil in winter, and has a very large effect on the soil temperatures and permafrost dynamics (Westermann et al., 2013; Langer et al., 2013; Ekici et al., 2014b). Thus in this model development work we consider implementing the physical effects of moss and organic matter, and further improving the snow scheme in JULES.

An accumulation of heat near the surface in the model can be related to the heat sink of the deeper part of the soil: if the model does not simulate a deep soil column this heat sink is missing. Several studies have shown that a shallow soil column does not give realistic temperature dynamics (Stevens et al., 2007; Alexeev et al., 2007). Finally the resolution of the soil column affects the numerical accuracy of the simulation and also the precision to which the ALT can be resolved. The default configuration for JULES represents only the top 3 m of soil with 4 layers. Therefore, in this work the depth and resolution of the soil column is increased, including a thermal “bedrock” column at the base.

The impact of soil hydrology is also considered, showing that if the soil moisture were simulated correctly the simulations of soil temperature could be further improved. Soil temperatures are affected by the water content of the soil not only through its thermal properties but also via the latent heat of freezing, which slows down the rate of temperature change.

Simulations are performed of the Samoylov Island site in Siberia, adding each model development in turn. This shows the impact of the new processes and significant improvements to model performance and the representation of permafrost in JULES. Areas for future development are also clearly identified.

GMDD
8, 715–759, 2015

2 Methods

2.1 Model description (standard version)

JULES is a stand-alone land-surface model which is also used in the Hadley Centre coupled climate models (Best et al., 2011; Clark et al., 2011), and was originally based on the MOSES land surface scheme (Cox et al., 1999; Essery et al., 2003). It combines a sophisticated energy and water balance model with a dynamic vegetation model. JULES is a community model and available from http://www.jchmr.org/jules. The work discussed here builds upon JULES version 3.4.1.

JULES simulates the physical, biophysical and biochemical processes that control the exchange of radiation, heat, water and carbon between the land surface and the atmosphere. It can be applied at a point or over a grid, and requires a continuous time-series of atmospheric forcing data at a frequency of 3 h or greater. Each grid box can contain several different land-covers or "tiles", including a number of different plant functional types (PFT's) as well as non-vegetated tiles (urban, water, ice and bare soil). Each tile has its own surface energy balance, but the soil underneath is treated as a single column and receives aggregated fluxes from the surface tiles.

JULES uses a multi-layer snow scheme (described in Best et al., 2011), in which the number of snow layers varies according to the depth of the snow pack. Each snow layer has a prognostic temperature, density, grain size and water content. In the old, zero-layer snow scheme, the insulation from snow was incorporated into the top layer of the soil. This scheme is currently still used when the snow depth is below 10 cm.

The subsurface temperatures are modelled via a discretization of both heat diffusion and heat advection by moisture fluxes. The soil thermal characteristics depend on the moisture content, as does the latent heat of freezing and thawing. A zero-heat-flux condition is applied at the lower boundary. The soil hydrology is based on a finite difference approximation of Richards' equation (Richards, 1931), with the same vertical discretisation as the soil thermodynamics (Cox et al., 1999). JULES uses the Brooks and Corey (1964) relations to describe the soil water retention curve and calculate hy-

GMDD
8, 715–759, 2015

draulic conductivity and soil water suction. Soil hydraulic and thermal parameters are input to the model via an ancillary file. The default vertical discretisation is a 3 m column modelled as 4 layers, with thicknesses of 0.1, 0.25, 0.65 and 2 m.

The land surface hydrology scheme (LSH) simulates a deep water store at the base of the soil column and allows subsurface flow from this layer, and any other layers below the water table. Topographic index data is used to generate the wetland fraction and saturation excess runoff (Gedney and Cox, 2003).

JULES also includes a dynamic vegetation model, TRIFFID, which simulates vegetation competition to determine the grid-box fraction assigned to each PFT (Cox, 2001). JULES may also be run with TRIFFID switched off and a fixed vegetation fraction, which was the case for the simulations in this paper, where the focus is on the physical processes.

2.2 Permafrost model developments

Model developments include the thermal effects of a surface moss layer, the thermal and hydrological effects of soil organic matter, a thermal "bedrock" column beneath the ordinary soil, and an improvement of the multilayer snow scheme to allow arbitrarily thin layers. The resolution and depth of the soil column is also increased. These improvements are described in detail in the following subsections.

2.2.1 Moss

The characteristics of moss will vary between different species and ecosystems, but all mosses will insulate the soil. Therefore the thermal conductivity of the soil was modified to represent this insulating layer. Its purpose in these simulations is to give a somewhat generic representation of the thin layer of moss-rich vegetation which is abundant in the Arctic. Although any vegetation layer in JULES has an insulating effect thanks to the canopy heat capacity (Best et al., 2011), this new type is necessary because the current PFT's are not appropriate for Arctic tundra.

GMDD
8, 715–759, 2015

The thermal conductivity of moss depends on its water content. For simplicity we assume that the moss layer coincides with the top layer of the soil, and thus has the same hydraulic suction. The water content is then calculated from the suction using the Brooks and Corey (1964) equation,

$$\frac{\theta_{\mathrm{moss}}}{\theta_{\mathrm{sat,moss}}} = \left(\frac{\psi}{\psi_{\mathrm{sat,moss}}}\right)^{-b_{\mathrm{moss}}}, \tag{1}$$

where θ is the volumetric water content, ψ is the soil water suction, b is the exponent and the subscript "sat" refers to the values at saturation. The following hydraulic parameters were used for moss (Beringer et al., 2001): $b_{\mathrm{moss}} = 1$, $\psi_{\mathrm{sat,moss}} = 0.12\,\mathrm{m}$, $\theta_{\mathrm{sat,moss}} = 0.9$.

The dependence of moss thermal conductivity on water content was measured by Soudzilovskaia et al. (2013). We choose the representative values for the saturated conductivity of $0.5\,\mathrm{W\,m^{-1}\,K^{-1}}$ and dry conductivity $0.06\,\mathrm{W\,m^{-1}\,K^{-1}}$, and linearly interpolate between the two depending on the moisture content (Eq. 1). These are also consistent with the values given for organic soils in Williams and Smith (1991).

The user can choose the thickness of the moss layer; the default value is 5 cm. The thermal conductivity of the top 5 cm of soil is then modified according to the parameters above. This is applied to a fraction of the gridbox depending on a variable representing the percentage cover of moss.

2.2.2 Organic soils

Organic soils were previously considered in JULES by Dankers et al. (2011), who concluded that their effects were small. In this paper, however, we use an improved implementation of their impact.

As in Dankers et al. (2011) the volumetric fraction of organic soil, f_{org}, was used to modify the soil properties to include the effects of organic matter. f_{org} was estimated as a vertical profile using observations of organic carbon at different depths. Soil carbon

GMDD
8, 715–759, 2015

observations were available in $kg\,m^{-3}$, which were converted to a volumetric fraction using literature values for the density ($800\,kg\,m^{-3}$) and porosity (Dankers et al., 2011, Table 2), of organic matter.

For some of the soil properties, the organic fraction was used to provide a linear weighting of organic and mineral characteristics (Appendix A, Eqs. A1, A4, A7), as in Dankers et al. (2011) and other similar work. However, the saturated hydraulic conductivity, dry thermal conductivity and saturated soil water suction were calculated using a more appropriate non-linear aggregation (Appendix A, Eqs. A2, A3, A8). As a result, the organic components of the dry thermal conductivity and saturated water suction have a larger effect than if they were calculated via a linear weighted average. See Appendix A for details. New soil properties, which include the effects of organic matter, may now be input to JULES via an updated soil ancillary file.

The current parametrisation of saturated thermal conductivity in JULES (Dharssi et al., 2009) restricts the values to those appropriate for mineral soils. Organic soils have a much lower saturated thermal conductivity, so it was necessary to modify the Dharssi parametrisation to take account of this.

The thermal conductivity of dry soil (λ_{dry}) is input to JULES via the ancillaries, and the saturated thermal conductivity is calculated in the model, depending on the fraction of the soil moisture that is currently frozen. The actual value of thermal conductivity is then calculated by interpolating between the dry and saturated conductivities depending on the water content. The literature values used in JULES for the dry thermal conductivity are $0.25\,W m^{-1}\,K^{-1}$ for clay soils and $0.3\,W m^{-1}\,K^{-1}$ for sandy soils, and saturated conductivity of 1.58 and $2.2\,W m^{-1}\,K^{-1}$ respectively (for unfrozen soils) (Williams and Smith, 1991, Table 4.1).

For organic soils, the dry conductivity is approximately $0.06\,W m^{-1}\,K^{-1}$ and the saturated conductivity $0.5\,W m^{-1}\,K^{-1}$ (Williams and Smith, 1991). However, using Dharssi's method the minimum value for saturated conductivity is $1.58\,W m^{-1}\,K^{-1}$. It was therefore necessary to implement a parametrisation of saturated thermal conductivity that extends to the appropriate values, for which a smooth curve was fitted to the data (Ap-

GMDD
8, 715–759, 2015

pendix A, Eq. A11). The two curves are shown on Fig. 1. The conductivities for mineral soils will be slightly different in the new formulation, but this difference will be small, and well within the uncertainty of the literature values.

Note that the same thermal conductivity values are used for both moss and organic soil. This is consistent with the fact that, for example in peat soils, the layer of living moss can be almost indistinguishable from the surface organic layer. One good reason for treating them separately, however, is that moss can also grow in places without a pronounced organic layer.

2.2.3 Bedrock

An extra column was added to the base of the hydrologically active soil column in JULES. This column represents bedrock, with no hydrological processes, as these can be assumed to be insignificant below a certain depth. This allows the representation of a deep soil column without a large computational load. Heat diffusion is the only process that is simulated:

$$C_{\text{deep}} \frac{\partial T_{\text{s,deep}}}{\partial t} = \lambda_{\text{deep}} \frac{\partial^2 T_{\text{s,deep}}}{\partial z^2}, \tag{2}$$

where $T_{\text{s,deep}}$ is the temperature in the deep soil column, t is time and z is vertical depth. This is discretized to first order as follows:

$$C_{\text{deep}} \frac{T_{\text{s,deep}}(i+1,n) - T_{\text{s,deep}}(i,n)}{\delta t} = \lambda_{\text{deep}} \frac{T_{\text{s,deep}}(i,n+1) - 2T_{\text{s,deep}}(i,n) + T_{\text{s,deep}}(i,n-1)}{\mathrm{d}z_{\text{deep}}^2} \tag{3}$$

where i indexes the timesteps and n indexes the vertical layers. This uses a constant heat capacity, C_{deep}, and thermal conductivity, λ_{deep}, which may be set by the user. The default values are $C_{deep} = 2.1 \times 10^6\,\mathrm{JK^{-1}m^{-3}}$ and $\lambda_{deep} = 8.6\,\mathrm{Wm^{-1}K^{-1}}$ (the properties of the soil solids in sand from Beringer et al. (2001), and very close to the values for quartz in Williams and Smith, 1991). By default, the vertical layer thickness is $dz_{deep} = 0.5\,\mathrm{m}$, with 100 layers, resulting in an extra 50 m soil column, but the user can also set these values. In most models the deep soil is not so finely resolved – in fact it is often represented as a single thick layer, but since the heat diffusion is so computationally light, there is no reason not to resolve the dynamics more accurately.

In the hydrologically active soil column an implicit solution is used for the temperature increments, but for bedrock the explicit solution is sufficient since temperature changes are slow and there are no freeze–thaw processes to consider. The heat flux across the boundary with the base of the hydrologically active soil column is

$$\text{heat flux} = \lambda_{base} \frac{(T_s(i,N) - T_{s,deep}(i,1))}{0.5(dz_{deep} + dz(N))} \tag{4}$$

where the thermal conductivity, λ_{base}, is an interpolation between the bottom layer of the hydrological column and the top layer of the bedrock column. Here N is the number of soil hydrological layers, which interface with the bedrock column. The heat flux at the base of the bedrock column is set to zero by default, but could be set to the geothermal heat flux in future versions.

2.2.4 Improved snow scheme

The original release of JULES included the same simple snow model as in the MOSES land surface scheme (Cox et al., 1999) and the HadCM3 climate model. In this, snow on the ground was represented by a modification of the properties of the surface layer in the soil model. The multi-layer snow model described by Best et al. (2011) was introduced as an option in JULES version 2.1 and was found to give significantly improved predictions of soil temperatures under deep snow (Burke et al., 2013), but the old snow model was retained for shallow snow of less than 10 cm depth to avoid numerical instabilities. For this study, a modification has been implemented that allows shallow snow

GMDD
8, 715–759, 2015

to be represented by a distinct model layer. This is done by calculating the heat flux into the snow or soil surface according to the temperature gradient between the surface and a fixed depth below the surface. The snow layer temperature is stepped forward in time using the backward Euler method, which remains stable for an infinitesimal layer thickness.

2.2.5 Increased soil resolution and depth

The hydrologically active soil column is run in 3 different configurations, beginning with the standard 4-layer configuration, with layer thicknesses 0.1, 0.25, 0.65 and 2.0 m. The second configuration increases the soil resolution without increasing the depth, having 14 layers in 3 m of soil. The layer thicknesses start at 0.05 m and increase with depth according to the function $dz_n = 0.05n^{0.75}$. Finally the high-resolution column is extended to 10 m with a total of 28 layers, following the same function for dz_n.

2.3 Samoylov Island site information

Point-scale simulations were carried out using data from Samoylov Island field site in the Lena river delta, Siberia. Figure 2 shows the location of Samoylov Island in the context of the whole Arctic permafrost region. There is a large quantity of data available from this site, making it a good site for detailed process evaluation (e.g., Yi et al., 2014). The landscape is formed of ice-wedge polygonal tundra with ponds and thermokarst lakes. There is an abundance of mosses and organic soil, so including the model developments described above has a notable impact on the JULES simulations. A typical soil profile is shown in Fig. 3b, highlighting the moss and organic layers. Figure 3a shows an aerial view of the monitoring site, including the meteorological station, soil temperature monitoring and active layer monitoring grid (only polygon centre points are highlighted as these data are used for evaluation). A detailed description of the site may be found in Boike et al. (2013).

GMDD
8, 715–759, 2015

2.3.1 Forcing data

The meteorological driving data were prepared using observations from the site combined with reanalysis data for the grid cell containing the site. For the period 1901–1979, Water and Global Change forcing data (WFD) was used (Weedon et al., 2010, 2011). This is a meteorological forcing dataset based on ERA-40 reanalysis (ECMWF, 2006), with corrections generated from Climate Research Unit (CRU) (Mitchell and Jones, 2005) and Global Precipitation Climatology Centre (GPCC) data (http://gpcc.dwd.de). Data is provided at half-degree resolution for the whole globe at 3 hourly time resolution from 1902–2001. For the period 1979–2010, WATCH Forcing Data Era-Interim (WFDEI) was used (Weedon, 2013). This is produced using the same techniques as the WFD but is instead based on the Era-Interim reanalysis data (ECMWF, 2009), and covers the period 1979–2012. For the time periods where observed data were available, correction factors were generated by calculating monthly biases relative to the WFDEI data. These corrections were then applied to the time-series from 1979–2010 of the WFDEI data. The WFD before 1979 was then corrected to match this data and the two datasets were joined at 1979 to provide gap-free 3 hourly forcing from 1901–2010.

Meteorological station observations were used for all variables except snowfall, which was estimated from the observed snow depth by treating increases in snow depth as snowfall events with an assumed snow density of 180 $kg\,m^{-3}$. Snow depth observations are available daily from 2002–2013, although with some missing years. These reconstructions were then used to provide correction factors to WFDEI and WFD. This leads to a more realistic snow depth in the model than using direct precipitation measurements, due to wind effects and the difficulty of accurately measuring snowfall.

GMDD
8, 715–759, 2015

2.3.2 Soil and land-cover characteristics

The land characteristics were chosen to represent a depressed polygon center, and the evaluation data (soil temperatures, moisture etc.) were also taken from polygon center measurements (see Fig. 3a).

The mineral soil is a sandy loam and was assumed to have 50 % silt, 45 % sand, 5 % clay, which is consistent with the information in Boike et al. (2013). The soil properties were calculated using the Cosby et al. (1984) relations. Site-specific organic carbon quantities are given in Zubrzycki et al. (2013), but there is significant heterogeneity, with values for polygon centres ranging between 3 and 85 $\mathrm{kg\,m^{-3}}$. The mean values of 25 $\mathrm{kg\,m^{-3}}$ of organic carbon above 30 cm and 35 $\mathrm{kg\,m^{-3}}$ from 30 cm to 1 m were used, giving a volumetric fraction f_{org} between 0.4 and 0.6. Following the model set-up used in (Langer et al., 2013), organic carbon below 1 m was taken as zero. The transition between carbon quantities above and below 30 cm was smoothed into a curve. Organic properties were then combined with the mineral properties as in Sect. 2.2.2.

To verify this parametrization of organic soil properties in JULES we compare the resulting thermal properties with those in Langer et al. (2011a, b). We compare saturated values in JULES with values for saturated peat. In JULES the thermal conductivity is consistent with the Langer values, lying between 0.7–0.9 $\mathrm{W\,m^{-1}\,K^{-1}}$ when thawed and between 1.9–2.1 $\mathrm{W\,m^{-1}\,K^{-1}}$ when frozen. The values from Langer et al. (2011a, b) are $0.72 \pm 0.08\,\mathrm{W\,m^{-1}\,K^{-1}}$ (thawed) and $1.92 \pm 0.19\,\mathrm{W\,m^{-1}\,K^{-1}}$ (frozen). The heat capacity in JULES is 3.5–3.8 $\mathrm{MJ\,m^{-3}\,K^{-1}}$ (thawed) and 2.2–2.3 $\mathrm{MJ\,m^{-3}\,K^{-1}}$ (frozen), which is again close to the Langer values of $3.8 \pm 0.2\,\mathrm{MJ\,m^{-3}\,K^{-1}}$ (thawed) and $2.0 \pm 0.05\,\mathrm{MJ\,m^{-3}\,K^{-1}}$ (frozen), although the heat capacity when frozen is a little too high in JULES, this is a reasonable level of consistency given the high spatial variability in soil properties.

The vegetation at Samoylov is composed predominantly of mosses, along with grasses and small shrubs at about 10 % coverage. The land-cover in JULES was taken as 10 % grass with a height of 10 cm. Moss cover was set to 90 % (or 90 % bare soil in simulations without moss).

GMDD
8, 715–759, 2015

For simulations with higher-resolution and deeper soil, the set-up is described in Sect. 2.2.5. The new bedrock routine was also used (Sect. 2.2.3), adding a futher 50 m heat sink to the base of the soil. Samoylov Island sits above a deep river deposit, so the deep soil is composed of silt deposits. The estimated parameters for the deep soil are approximately $C_{deep} = 2.1\,MJ\,m^{-3}\,K^{-1}$ and $\lambda_{deep} = 2\,Wm^{-1}\,K^{-1}$, so these values were used for the bedrock column in JULES (Boike et al., 2013).

The improved snow scheme was included, along with a change of the fresh snow density in all simulations from the default value of 100 to 130 $kg\,m^{-3}$, to better match the observed snow density and depth. The fresh snow density applies when the snow first reaches the ground, after which it undergoes standard compaction processes, meaning that a higher fresh snow density will lead to a higher snow density year-round. In test runs the mean simulated density over all snow-covered periods was around 190 $kg\,m^{-3}$ (compared with 165 $kg\,m^{-3}$ with the default fresh snow density). It is possible that this estimate is still too low, since the observed density for a polygon centre is around 230 $kg\,m^{-3}$. However, 190 $kg\,m^{-3}$ is close to the spatial average given in Boike et al. (2013) and this is also approximately consistent with the assumed value of 180 $kg\,m^{-3}$ used to create the driving data. This is considered further in Sect. 3.2.

The LSH scheme was also switched on (see Sect. 2.1). This scheme adds a deep water store at the base of the soil and thus improves the water-holding capacity of the soil.

2.3.3 Simulation set-up

Simulations were performed first for the standard version of JULES using just mineral soil (std). The developments of increased soil discretisation (min14l), deeper soil (minD), organic soil properties (orgD), moss insulation (orgmossD) and the improved snow scheme (orgmossDS) were then systematically introduced (see Table 1), with the final simulation containing all of the model improvements (orgmossDS). The simulations labelled “$\rho_{fresh} = 170$” and “*Saturated*” in Table 1 are discussed in Sect. 3.2.

The simulations were spun-up for 200 years using the first 10 years of driving data (starting at 2 January 1901), by which point the soil temperatures and water contents were stable. They were then run from 1901 until the end of 2010.

2.4 Calculating active layer thickness (ALT)

Commonly used methods of calculating ALT in land-surface models make use of the soil temperatures, either by taking the depth of the deepest layer that is above 0 °C, or an interpolation of soil temperatures to find the depth of 0 °C, see for example Koven et al. (2012); Lawrence et al. (2012). However, this method is limited by the vertical discretisation. In JULES, when a given layer is freezing or thawing, the temperature of the layer remains very close to 0 °C for the duration of freeze–thaw, with the consequence that any interpolation puts the thaw depth very close to the centre of the layer. However, more information may be extracted from JULES by outputting the frozen and unfrozen water contents in the layer. In this paper, the ALT is calculated by taking the unfrozen water fraction, θ_u, in the deepest layer that has begun to thaw, and assuming that this same fraction of the soil layer has thawed. This is represented by the following equation:

$$\mathrm{ALT} = \sum_{i=1,n} \mathrm{d}z_i + \frac{\theta_{u,n+1}}{\theta_{u,n+1} + \theta_{f,n+1}} \mathrm{d}z_{n+1}, \tag{5}$$

where n is the deepest layer that has completely thawed ($\theta_{\mathrm{f},n} = 0$, where θ_{f} is the frozen water fraction). This gives significantly more precise estimates than the usual temperature interpolation.

Figure 4 shows an example of the thawing period in 2006 for one of the JULES simulations (orgmossDS, Table 1), where the thaw begins too early but the maximum depth is well simulated. The temperature interpolation method uses a linear interpolation to find the depth of 0 °C. It is clear that this method produces thaw depth in a series of steps corresponding to the JULES layers. The new method based on fraction of un-

GMDD
8, 715–759, 2015

frozen soil moisture gives a much smoother curve, which corresponds better to the observations.

3 Results and discussion

3.1 Soil temperatures and ALT

Figure 5 shows the simulated ALT at Samoylov over the 11 year period 2000–2010. It is clear that many of the new processes in the model reduce the ALT, with the final simulation including deep soil, moss, organic properties and the new snow scheme (orgmossDS) bringing the simulated ALT very close to the observations. In orgmossDS the ALT falls within the range of observations for every year where measurements are available. A significant bias of over 1 m for the standard JULES set-up (std) has been removed by including these model developments.

Comparing the first two simulations, std and min14l, the mean ALT is reduced by 0.2 m when soil resolution is increased. The base layer in std is 2 m thick, and the thaw depth consistently reaches almost to the centre of this layer, although in some years earlier in the simulation (not shown) the thaw reaches only the 3rd model layer and thus the ALT changes by approximately 0.5 m in one year, which is unrealistic behaviour.

A comparison of shallow and deep simulations, both with high resolution (min14l and minD on Fig. 5) demonstrates that there is a small but significant reduction in bias when the depth of the soil column is increased to 10 m and bedrock is added. In this case the mean ALT is reduced by 0.13 m.

The addition of the organic soil parametrisation has the single biggest impact on the ALT in these simulations. The mean ALT in minD is 1.03 m, and in orgD it is 0.49 m, a reduction of over half a metre. Moss on its own also has a large impact, reducing the mean ALT by 0.35 m from minD to minmossD. However, the effects are non-linear: comparing orgD and orgmossD, the mean ALT is reduced by only 0.17 m by the addition of moss.

GMDD
8, 715–759, 2015

The ALT depends on the maximum soil temperatures in summer, but it is important to simulate the correct soil temperatures for the whole year and the whole soil column. Table 2 shows some key performance metrics for the soil temperatures at different depths, most of which are significantly improved in the final simulation (orgmossDS). This shows that although the changes to the snow scheme have very little effect on the ALT, they reduce the root mean square error (RMSE) in upper soil temperatures from 4.1 to 3.4 °C, which is a significant improvement.

The simulated active layer temperatures in the mineral soil simulations (std, min14l and minD), shown in Table 2, are too warm (≈ 2 °C), and the annual cycle is much too large. This is consistent with the large-scale biases in JULES discussed in Sect. 1. The addition of organic soils and moss reduces the mean active layer temperature and annual cycle to more realistic values. The changes to the snow scheme then increase the active layer temperature by 1.2 °C, but the temperature bias is still less than 1 °C and the annual cycle bias is reduced from 30 % to less than 10 % in orgmossDS.

Considering the deep soil temperatures in Table 2, organic soils and moss have a cooling effect, which is offset by a warming due to the change in snow scheme (this is also true at 32 cm depth). The temperature biases are more negative (or less positive) deeper in the soil than they are at the surface, and the annual cycles also have biases that are inconsistent at different depths. This suggests that the profile of soil temperatures is not entirely realistic in the simulations. Further measurements of deep soil properties at the site would allow a more detailed analysis of this.

Figure 6a and b shows the active layer soil temperatures in more detail, showing the combined effect of the model improvements. Temperatures are shown for both the whole active layer (Fig. 6a) and for the single depth of 32 cm (Fig. 6b). The limitation of the lower-resolution standard JULES set-up (std) is clear on Fig. 6a, where the soil temperature changes in a series of steps, whereas it is much smoother in both the observations and the other simulations.

Figure 6b shows that the improved model matches the observed soil temperatures much better in summer, and somewhat better in the shoulder seasons (spring and

GMDD
8, 715–759, 2015

autumn). Comparing minD with orgmossD shows that organic soils and moss have the main impact on summer soil temperatures. Comparing orgmossD and orgmossDS shows that the snow scheme has the greatest effect during the shoulder seasons.

At 32 cm depth, the RMSE in the warmest months (August–September) is reduced from 4.0 °C in the minD simulation to just 0.7 °C in orgmossDS. This suggests that the most important processes for the summer have been identified and included, namely the insulating effects of moss and organic soils. However, the temperatures in snow-covered seasons are much more difficult to simulate, with the RMSE for the other months reduced from 5.3 °C in minD to 3.9 °C in orgmossDS, which is a significant reduction but not nearly so large as for the summer. One reason for this is that snow varies dynamically on short timescales, which strongly affects the energy balance. In contrast, processes that affect the summer temperatures are relatively static – for example, the organic content of the soil will change very slowly (peat growth of around 2 mm per year is observed at the site). Snow will be considered further in Sect. 3.2.

3.2 Snow and soil moisture

The largest remaining errors in soil temperatures in the final simulation (orgmossDS) occur during the winter and shoulder seasons (see Fig. 6b). Figure 7 shows the observed and simulated snow depth over the same time period as Fig. 6b. It is clear that in winter 2003–2004, when the mid-winter soil temperatures are simulated fairly accurately, the snow depth is below that observed, whilst in winter 2004–2005, the snow depth is close to the observations but the soil temperatures are too warm. This suggests that the simulated snow density is too low. The snow density determines the thermal conductivity, which, combined with the snow depth, is used to calculate the heat flow between air and soil.

A further simulation was performed, increasing the fresh snow density even more from 130 to 170 kg m^{-3} (see Table 1). This increased the mean snow density that was simulated in JULES from around 190 to 220 kg m^{-3}, which matches more closely with the observational estimate specifically for polygon centres, which is in the region of 230 kg m^{-3} (Boike et al., 2013).

Figure 8 shows the effect of increasing snow density. The soil is now too cold in winter 2003–2004, which is consistent with there being too little snow. In winter 2004–2005, where snow depths are more realistic, the soil temperatures match better with those observed. During the coldest months (January–March), there is a strong correlation of approximately 0.85 between the error in snow depth and the error in soil temperature, for both simulations. However, the linear regression line crosses a long way above the origin in orgmossDS (4.3 °C), whereas when the fresh snow density is higher it passes closer to the origin (1.8 °C) – see Fig. 8. For these months, using $\rho_{\text{fresh}} = 170$ kg m^{-3} reduces the RMSE in soil temperature from 3.9 to 2.4 °C. However, the whole-year RMSE in soil temperature is increased from 3.4 to 3.7 °C, mainly because of differences in temperatures in the shoulder seasons, in particular during the freeze-up period in autumn, where the simulated zero-curtain length is too short (zero-curtain is the period for which the soil remains at or close to 0 °C during freeze or thaw). The end of the freeze-up happens on average 30 days too early in orgmossDS, and when the snow density is increased it is even earlier, on average 42 days before the observed freeze-up date.

The zero-curtain duration is determined by the latent heat associated with freeze–thaw. In reality, polygon centers tend to be saturated (Boike et al., 2013). If there is not enough soil moisture, some latent heat will be missing, reducing the zero-curtain length. Figure 9 compares the volumetric soil moisture content in the observations and simulations. It is clearly improved in the organic soil simulations (orgmossD, orgmossDS) compared with the mineral soil simulations (std, minD), but there is still too little soil moisture, partly because the porosity is too low and partly because the soil does not always stay saturated. The offset timings of freeze and thaw are clearly seen, showing that the timing of thaw is greatly improved in orgmossD and orgmossDS, but there is little effect on the time of the freeze. Note that the unfrozen soil moisture con-

GMDD
8, 715–759, 2015

tent in winter is higher than the observations, which suggests the hydraulic parameters may need some refinement.

In order to investigate the soil moisture effect, a simulation was performed in which the soil was kept saturated all year round, and the organic matter content in the upper soil layers was increased to 45 $kg\,m^{-3}$ to increase the porosity to match better with the observations ("*Saturated*" in Table 1). As a result, the thermal conductivity and heat capacity generally fall within the uncertainty of the values in Langer et al. (2011a, b), although the frozen heat capacity is increased with a maximum value of 2.4 $MJ\,m^{-3}\,K^{-1}$, which is 20 % greater than the values in Langer et al. (2011b). The simulation results are shown in Fig. 10.

Figure 10 shows a great improvement in the zero-curtain length, with the mean difference between the simulated and observed freeze-up now being only 13 days (instead of 30 in orgmossDS). The overall RMSE for the upper soil temperatures is reduced further from 3.4 to 2.7 °C, and the deep soil temperatures are also improved (see "*Saturated*" in Table 2). The summer soil temperatures are actually a little warmer and in fact this reduces the RMSE for August–September temperatures (at 32 cm) slightly from 0.7 to 0.6 °C. Figure 10a shows that the timeseries of unfrozen soil moisture is also greatly improved. These improvements highlight the need for more work on soil hydrology.

The simulation where the soil is held saturated is now a great improvement on the original mineral soil simulation, with RMSE at 32 cm reduced by almost half. However, the zero-curtain still falls short by nearly 2 weeks, and the mid-winter temperatures still differ significantly from observations, especially for winter 2003–2004. The difference of winter temperatures is likely due to the driving data, which does not always result in the correct snow depth in the model, nor the timing of snowfall and snowmelt (see Fig. 7). In reality, snow depth at Samoylov does not correspond very closely to snowfall, as it depends strongly on wind-redistribution. This is a difficult problem to solve for a 1-D model such as JULES. The problem of zero-curtain duration, however, may also be related to the snow density, and there is scope to improve this in the model. Accord-

GMDD
8, 715–759, 2015

ing to the parameterization used in the Crocus snowpack model, which depends on temperature and wind speed (Vionnet et al., 2012), the fresh snow density should be much lower than 170 $kg\,m^{-3}$ for this site. This would give more snow insulation during the freeze-up period, but the simulated mid-winter snow density in JULES would then be too low. This could be addressed by including compaction processes in the model that are currently not represented, such as wind compaction and temperature-gradient metamorphosis, both of which are potentially important (Sturm and Holmgren, 1998; Vionnet et al., 2012).

4 Conclusions and future work

Improvements have been made to the physical representation of permafrost in the JULES land-surface model. Additional processes represented include an insulating moss layer, the physical properties of organic soil, and a bedrock column. In addition, the representation of snow and discretization of the soil have been modified. These developments have significantly improved soil temperatures and ALT. The importance of simulating a deep and well-resolved soil column is seen in the reduction of ALT by 0.33 m between the standard 3 m version (std) and a model version with a 10 m soil column and bedrock (minD). The importance of mosses and organic soils is then seen in the further reduction of ALT by 0.71 m. The RMSE in summer soil temperatures is now less than 1 °C. Deeper soil is also important for studying the full permafrost column, and previous work has shown that a shallow soil column does not give realistic permafrost dynamics, see e.g. Lawrence et al. (2008). The improvement to the snow model is essential for simulating soil temperatures in the shoulder seasons.

Samoylov is a particularly complex site to simulate because there is a strong temperature cycle, it is very cold, there are strong wind effects and small-scale landscape variability. However, it is typical of low-lying tundra regions, so it is important that JULES can simulate this type of landscape.

GMDD
8, 715–759, 2015

The *Saturated* simulation improves further on orgmossDS and indicates that the hydrology is very important for the soil temperatures, particularly the timing of freeze-up, which is improved from 30 to only 13 days too early. This simulation does not run the full model as the water fluxes are set to zero, but it shows that hydrological processes in JULES require further work. There are some remaining differences in soil temperature between this simulation and observations, which are discussed in Sect. 3.2. These differences appear to be related to the snow, and indicate that this also requires further work. In particular, the fresh snow density required to obtain the correct mid-winter snow density in the model is too high, suggesting that it is necessary to include more snow compaction processes in JULES.

Another area in need of further development is the vegetation. There is no appropriate tundra vegetation type in JULES and no specific high-latitude PFT's. The moss cover represented here is a first step towards simulating tundra vegetation, however this represents only the physical effects of a constant layer of moss, leaving much more work to be done, for example on growth, carbon cycling, and on other types of vegetation.

We believe that we have significantly improved the representation of permafrost processes in JULES, providing generic model improvements that could be adopted in other GCM land-surface schemes. However, this is still a work in progress for the whole community. Even if a model simulates the right processes in a 1-D column, scaling these up to represent sub-grid heterogeneity in a large grid-box is still an open problem (Muster et al., 2012; Langer et al., 2013). In most global land-surface models, only vertical processes are simulated, meaning the lateral flow of heat and water, and blowing snow are all omitted. Techniques to include these processes are currently under development (e.g., Tian et al., 2012; Essery and Pomeroy, 2004; Yi et al., 2014). Of course on the large scale, models are still heavily constrained by the availability and uncertainty of observational data.

GMDD
8, 715–759, 2015

5 Code availability

The model developments are available in JULES branches created by S. Chadburn (sec234) and E. Burke (hadea) on PUMA (https://puma.nerc.ac.uk/svn/JULES_svn/JULES/branches/dev/). A password can be requested for access (see https://jules.jchmr.org). If you would like us to send you the code, please contact us.

Appendix A: Details of organic soil parameterisation

Using an organic fraction, f_{org}, organic and mineral soil properties are combined as follows:

$$b = (1 - f_{\mathrm{org}})b_{\mathrm{m}} + f_{\mathrm{org}}b_{\mathrm{o}} \tag{A1}$$

$$\Psi_{\mathrm{sat}} = \Psi_{\mathrm{sat,m}}^{1-f_{\mathrm{org}}}\Psi_{\mathrm{sat,o}}^{f_{\mathrm{org}}} \tag{A2}$$

$$K_{\mathrm{s}} = K_{\mathrm{s,m}}^{1-f_{\mathrm{org}}}K_{\mathrm{s,o}}^{f_{\mathrm{org}}} \tag{A3}$$

$$\theta_{\mathrm{sat}} = (1 - f_{\mathrm{org}})\theta_{\mathrm{sat,m}} + f_{\mathrm{org}}\theta_{\mathrm{sat,o}} \tag{A4}$$

$$\theta_{\mathrm{crit}} = \theta_{\mathrm{sat}}\left(\frac{\Psi_{\mathrm{sat}}}{3.364}\right)^{1/b} \tag{A5}$$

$$\theta_{\mathrm{wilt}} = \theta_{\mathrm{sat}}\left(\frac{\Psi_{\mathrm{sat}}}{152.9}\right)^{1/b} \tag{A6}$$

$$C_{\mathrm{dry}} = (1 - f_{\mathrm{org}})C_{\mathrm{dry,m}} + f_{\mathrm{org}}C_{\mathrm{dry,o}} \tag{A7}$$

$$\lambda_{\mathrm{dry}} = \lambda_{\mathrm{dry,m}}^{1-f_{\mathrm{org}}}\lambda_{\mathrm{dry,o}}^{f_{\mathrm{org}}} \tag{A8}$$

Subscripts m and o denote values for mineral and organic soils, respectively. K_{s} is the hydraulic conductivity at saturation, θ_{crit} and θ_{wilt} are the moisture contents for the critical point and wilting point, and C_{dry} and λ_{dry} are thermal properties: heat capacity

GMDD
8, 715–759, 2015

and thermal conductivity of dry soil. The properties for organic soils are as in Dankers et al. (2011), Table 2. Some of these parameters are given as 3 different values for different vertical layers of the soil. The division between layers was taken at 0.3 and 1 m.

While the dry thermal conductivity, λ_{dry}, is input to JULES, the saturated thermal conductivity is calculated in the model. The preferred parametrisation of saturated thermal conductivity in the standard version of JULES (Dharssi et al., 2009) is as follows:

$$\lambda_{\mathrm{sat}} = \lambda_{\mathrm{sat0}} \frac{\lambda_{\mathrm{wat}}^{f_{\mathrm{wat}}\theta_{\mathrm{sat}}} \lambda_{\mathrm{ice}}^{f_{\mathrm{ice}}\theta_{\mathrm{sat}}}}{\lambda_{\mathrm{wat}}^{\theta_{\mathrm{sat}}}} \tag{A9}$$

where

$$f_{\mathrm{wat}} = \theta_{\mathrm{u}}/(\theta_{\mathrm{u}} + \theta_{\mathrm{f}}); f_{\mathrm{ice}} = \theta_{\mathrm{f}}/(\theta_{\mathrm{u}} + \theta_{\mathrm{f}})$$

where θ_{u} is the volumetric unfrozen water content and θ_{f} is the volumetric frozen water content. λ_{sat0} is the saturated thermal conductivity when the soil is entirely unfrozen, given by

$$\lambda_{\mathrm{sat0}} = \left\{ \begin{array}{cc} 1.58 & \lambda_{\mathrm{dry}} < 0.25 \\ (1.58 + 12.4(\lambda_{\mathrm{dry}} - 0.25)) & 0.25 < \lambda_{\mathrm{dry}} < 0.3 \\ 2.2 & \lambda_{\mathrm{dry}} > 0.3 \end{array} \right\} \mathrm{W m^{-1} K^{-1}} \tag{A10}$$

This parameterisation is replaced with the following equation, which allows the saturated conductivity to take lower values appropriate to organic soils:

$$\lambda_{\mathrm{sat0}} = \left\{ \begin{array}{cc} 0.5 & \lambda_{\mathrm{dry}} < 0.06 \\ \frac{1.0 - 0.0134\ln(\lambda_{\mathrm{dry}})}{-0.745 - \ln(\lambda_{\mathrm{dry}})} & 0.06 < \lambda_{\mathrm{dry}} < 0.3 \\ 2.2 & \lambda_{\mathrm{dry}} > 0.3 \end{array} \right\} \mathrm{W m^{-1} K^{-1}} \tag{A11}$$

GMDD
8, 715–759, 2015
Improved physical permafrost dynamics in the JULES land surface model
S. Chadburn et al.

This was derived using the generic logarithmic function $(1 + a\ln(\lambda_{dry}))/(b + c\ln(\lambda_{dry}))$, using 3 free parameters, a, b and c to fit to the three available literature values, since this gives a smooth curve. Alternatively linear interpolation may be used, describing λ_{sat0} in two segments with a discontinuity in gradient at $\lambda_{dry} = 0.25\,\mathrm{W m^{-1} K^{-1}}$. There is little difference between the two methods and the smooth curve was chosen by virtue of its lack of discontinuity.

Author contributions. S. Chadburn and E. Burke developed moss, organic soil and bedrock representations in the model. R. Essery developed the improved snow scheme. J. Boike, M. Langer and M. Heikenfeld provided field data, images and knowledge of the Samoylov Island site. P. Friedlingstein and P. Cox provided initial ideas and oversight. S. Chadburn ran the simulations and wrote up the results.

Acknowledgements. The authors acknowledge financial support by the European Union Seventh Framework Programme (FP7/2007–2013) project PAGE21, under GA282700. E. J. Burke was supported by the Joint UK DECC/Defra Met Office Hadley Centre Climate Programme GA01101. M. Langer is also supported by a Post-Doctoral Research Fellowshop (A. v. Humboldt Foundation). Work was facilitated by a PAGE21 young researcher exchange grant. Thanks go to the Russian–German expedition team for logistical support during the Samoylov field work. Thanks to Niko Bornemann, Steffen Frey and Günter Stoof for data collection and compilation.

References

Alexeev, V. A., Nicolsky, D. J., Romanovsky, V. E., and Lawrence, D. M.: An evaluation of deep soil configurations in the CLM3 for improved representation of permafrost, Geophys. Res. Lett., 34, L09502, doi:10.1029/2007GL029536, 2007. 719

Bekryaev, R. V., Polyakov, I. V., and Alexeev, V. A.: Role of polar amplification in long-term surface air temperature variations and modern Arctic warming, J. Climate, 23, 3888–3906, doi:10.1175/2010JCLI3297.1, 2010. 717

Beringer, J., Lynch, A. H., Chapin, F. S., Mack, M., and Bonan, G. B.: The representation of Arctic soils in the land surface model: the importance of mosses, J. Climate, 14, 3324–3335, doi:10.1175/1520-0442(2001)014<3324:TROASI>2.0.CO;2, 2001. 718, 722, 725

Best, M. J., Pryor, M., Clark, D. B., Rooney, G. G., Essery, R .L. H., Ménard, C. B., Edwards, J. M., Hendry, M. A., Porson, A., Gedney, N., Mercado, L. M., Sitch, S., Blyth, E., Boucher, O., Cox, P. M., Grimmond, C. S. B., and Harding, R. J.: The Joint UK Land Environment Simulator (JULES), model description – Part 1: Energy and water fluxes, Geosci. Model Dev., 4, 677–699, doi:10.5194/gmd-4-677-2011, 2011. 718, 720, 721, 725

Boike, J., Kattenstroth, B., Abramova, K., Bornemann, N., Chetverova, A., Fedorova, I., Fröb, K., Grigoriev, M., Grüber, M., Kutzbach, L., Langer, M., Minke, M., Muster, S., Piel, K., Pfeiffer, E.-M., Stoof, G., Westermann, S., Wischnewski, K., Wille, C., and Hubberten, H.-W.: Baseline characteristics of climate, permafrost and land cover from a new permafrost observatory in the Lena River Delta, Siberia (1998–2011), Biogeosciences, 10, 2105–2128, doi:10.5194/bg-10-2105-2013, 2013. 726, 728, 729, 734

Brooks, R. and Corey, A.: Hydraulic Properties of Porous Media, Colorado State University Hydrology Papers, Colorado State University, available at: http://books.google.co.uk/books?id=F_1HOgAACAAJ (last access: 27 January 2015), 1964. 720, 722

Brown, J., Ferrians Jr, O. J., Heginbottom, J., and Melnikov, E.: Circum-arctic map of permafrost and ground ice conditions, National Snow and Ice Data Center, available at: http://nsidc.org/data/docs/fgdc/ggd318_map_circumarctic (last access: 27 January 2015), 1998. 751

Brown, J., Nelson, F. E., and Hinkel, K. M.: The circumpolar active layer monitoring (CALM) program: research designs and initial results, Polar Geography, 3, 165–258, 2000. 718

Burke, E., Dankers, R., Jones, C., and Wiltshire, A.: A retrospective analysis of pan Arctic permafrost using the JULES land surface model, Clim. Dynam., 41, 1025–1038, doi:10.1007/s00382-012-1648-x, 2013. 718, 725

Burke, E. J., Hartley, I. P., and Jones, C. D.: Uncertainties in the global temperature change caused by carbon release from permafrost thawing, The Cryosphere, 6, 1063–1076, doi:10.5194/tc-6-1063-2012, 2012. 717

Camill, P.: Permafrost thaw accelerates in boreal peatlands during late-20th century climate warming, Climatic Change, 68, 135–152, doi:10.1007/s10584-005-4785-y, 2005. 717

Christensen, T. R. and Cox, P.: Response of methane emission from arctic tundra to climatic change: results from a model simulation, Tellus B, 47, 301–309, doi:10.1034/j.1600-0889.47.issue3.2.x, 1995. 718

Clark, D. B., Mercado, L. M., Sitch, S., Jones, C. D., Gedney, N., Best, M. J., Pryor, M., Rooney, G. G., Essery, R. L. H., Blyth, E., Boucher, O., Harding, R. J., Huntingford, C., and Cox, P. M.: The Joint UK Land Environment Simulator (JULES), model description – Part 2:

GMDD
8, 715–759, 2015

Carbon fluxes and vegetation dynamics, Geosci. Model Dev., 4, 701–722, doi:10.5194/gmd-4-701-2011, 2011. 718, 720

Cosby, B. J., Hornberger, G. M., Clapp, R. B., and Ginn, T. R.: A statistical exploration of the relationships of soil moisture characteristics to the physical properties of soils, Water Resour. Res., 20, 682–690, doi:10.1029/WR020i006p00682, 1984. 728

Cox, P. M.: Description of the TRIFFID Dynamic Global Vegetation Model, Hadley Centre Technical Note 24, Hadley Centre, Met Office, Bracknell, UK, 2001. 721

Cox, P. M., Betts, R. A., Bunton, C. B., Essery, R. L. H., Rowntree, P. R., and Smith, J.: The impact of new land surface physics on the GCM simulation of climate and climate sensitivity, Clim. Dynam., 15, 183–203, doi:10.1007/s003820050276, 1999. 718, 720, 725

Dankers, R., Burke, E. J., and Price, J.: Simulation of permafrost and seasonal thaw depth in the JULES land surface scheme, The Cryosphere, 5, 773–790, doi:10.5194/tc-5-773-2011, 2011. 718, 722, 723, 739

Dharssi, I., Vidale, P., Verhoef, A., Macpherson, B., Jones, C., and Best, M.: New soil physical properties implemented in the Unified Model at PS18, Meteorology Research and Development technical report 528, Met. Office, UK, available at: http://www.metoffice.gov.uk/archive/forecasting-research-technical-report-528 (last access: 27 January 2015), 2009. 723, 739

Dyrness, C.: Control of depth to permafrost and soil temperature by the forest floor in black spruce/feathermoss communities, Pacific Northwest Forest and Range Experiment Station (Portland, Or.), 396, 1982. 719

ECMWF (European Center for Medium-Range Weather Forecasts): ECMWF ERA-40 Re-Analysis data, NCAS British Atmospheric Data Centre, available at: http://badc.nerc.ac.uk/view/badc.nerc.ac.uk__ATOM__dataent_ECMWF-E40 (last access: 27 January 2015), 2006. 727

ECMWF (European Center for Medium-Range Weather Forecasts): ECMWF ERA-40 Re-Analysis data, NCAS British Atmospheric Data Centre, available at: http://badc.nerc.ac.uk/view/badc.nerc.ac.uk__ATOM__dataent_12458543158227759 (last access: 27 January 2015), 2009. 727

Ekici, A., Beer, C., Hagemann, S., Boike, J., Langer, M., and Hauck, C.: Simulating high-latitude permafrost regions by the JSBACH terrestrial ecosystem model, Geosci. Model Dev., 7, 631–647, doi:10.5194/gmd-7-631-2014, 2014a. 718

Ekici, A., Chadburn, S., Chaudhary, N., Hajdu, L. H., Marmy, A., Peng, S., Boike, J., Burke, E., Friend, A. D., Hauck, C., Krinner, G., Langer, M., Miller, P. A., and Beer, C.: Site-level model intercomparison of high latitude and high altitude soil thermal dynamics in tundra and barren landscapes, The Cryosphere Discuss., 8, 4959–5013, doi:10.5194/tcd-8-4959-2014, 2014b. 719

Essery, R. and Pomeroy, J.: Vegetation and topographic control of wind-blown snow distributions in distributed and aggregated simulations for an Arctic tundra basin, J. Hydrometeorol., 5, 735–744, doi:10.1175/1525-7541(2004)005<0735:VATCOW>2.0.CO;2, 2004. 737

Essery, R., Best, M., Betts, R., and Taylor, C.: Explicit representation of subgrid heterogeneity in a GCM land surface scheme, J. Hydrometeorol., 4, 530–543, 2003. 720

Exbrayat, J.-F., Pitman, A. J., Zhang, Q., Abramowitz, G., and Wang, Y.-P.: Examining soil carbon uncertainty in a global model: response of microbial decomposition to temperature, moisture and nutrient limitation, Biogeosciences, 10, 7095–7108, doi:10.5194/bg-10-7095-2013, 2013. 717

Gedney, N. and Cox, P. M.: The sensitivity of global climate model simulations to the representation of soil moisture, J. Hydrometeorol., 4, 1265–1275, doi:10.1175/1525-7541(2003)004<1265:TSOGCM>2.0.CO;2, 2003. 721

Gouttevin, I., Krinner, G., Ciais, P., Polcher, J., and Legout, C.: Multi-scale validation of a new soil freezing scheme for a land-surface model with physically-based hydrology, The Cryosphere, 6, 407–430, doi:10.5194/tc-6-407-2012, 2012a. 718

Gouttevin, I., Menegoz, M., Dominé, F., Krinner, G., Koven, C., Ciais, P., Tarnocai, C., and Boike, J.: How the insulating properties of snow affect soil carbon distribution in the continental pan-Arctic area, J. Geophys. Res.-Biogeo., 117, G02020, doi:10.1029/2011JG001916, 2012b. 717

Jafarov, E. E., Marchenko, S. S., and Romanovsky, V. E.: Numerical modeling of permafrost dynamics in Alaska using a high spatial resolution dataset, The Cryosphere, 6, 613–624, doi:10.5194/tc-6-613-2012, 2012. 717

Khvorostyanov, D. V., Ciais, P., Krinner, G., and Zimov, S. A.: Vulnerability of east Siberia's frozen carbon stores to future warming, Geophys. Res. Lett., 35, L10703, doi:10.1029/2008GL033639, 2008. 717

Koven, C., Friedlingstein, P., Ciais, P., Khvorostyanov, D., Krinner, G., and Tarnocai, C.: On the formation of high-latitude soil carbon stocks: effects of cryoturbation and insulation by organic matter in a land surface model, Geophys. Res. Lett., 36, L21501, doi:10.1029/2009GL040150, 2009. 719

GMDD
8, 715–759, 2015

Improved physical permafrost dynamics in the JULES land surface model

S. Chadburn et al.

Koven, C. D., Ringeval, B., Friedlingstein, P., Ciais, P., Cadule, P., Khvorostyanov, D., Krinner, G., and Tarnocai, C.: Permafrost carbon–climate feedbacks accelerate global warming, P. Natl. Acad. Sci. USA, doi:10.1073/pnas.1103910108, 2011. 717

Koven, C. D., Riley, W. J., and Stern, A.: Analysis of permafrost thermal dynamics and response to climate change in the CMIP5 earth system models, J. Climate, 26, 1877–1900, doi:10.1175/JCLI-D-12-00228.1, 2012. 717, 730

Langer, M., Westermann, S., Muster, S., Piel, K., and Boike, J.: The surface energy balance of a polygonal tundra site in northern Siberia – Part 1: Spring to fall, The Cryosphere, 5, 151–171, doi:10.5194/tc-5-151-2011, 2011a. 728, 735

Langer, M., Westermann, S., Muster, S., Piel, K., and Boike, J.: The surface energy balance of a polygonal tundra site in northern Siberia – Part 2: Winter, The Cryosphere, 5, 509–524, doi:10.5194/tc-5-509-2011, 2011b. 728, 735

Langer, M., Westermann, S., Heikenfeld, M., Dorn, W., and Boike, J.: Satellite-based modeling of permafrost temperatures in a tundra lowland landscape, Remote Sens. Environ., 135, 12–24, doi:10.1016/j.rse.2013.03.011, 2013. 719, 728, 737

Lawrence, D. and Slater, A.: Incorporating organic soil into a global climate model, Clim. Dynam., 30, 145–160, doi:10.1007/s00382-007-0278-1, 2008. 718

Lawrence, D., Slater, A., Romanovsky, V., and Nicolsky, D.: Sensitivity of a model projection of near-surface permafrost degradation to soil column depth and representation of soil organic matter, J. Geophys. Res., 113, F02011, doi:10.1029/2007JF000883, 2008. 719, 736

Lawrence, D. M., Slater, A. G., and Swenson, S. C.: Simulation of present-day and future permafrost and seasonally frozen ground conditions in CCSM4, J. Climate, 25, 2207–2225, doi:10.1175/JCLI-D-11-00334.1, 2012. 730

Mitchell, T. D. and Jones, P. D.: An improved method of constructing a database of monthly climate observations and associated high-resolution grids, Int. J. Climatol., 25, 693–712, doi:10.1002/joc.1181, 2005. 727

Muster, S., Langer, M., Heim, B., Westermann, S., and Boike, J.: Subpixel heterogeneity of ice-wedge polygonal tundra: a multi-scale analysis of land cover and evapotranspiration in the Lena River Delta, Siberia, Tellus B, 64, 17301, doi:10.3402/tellusb.v64i0.17301, 2012. 737

Overland, J. E., Spillane, M. C., Percival, D. B., Wang, M., and Mofjeld, H. O.: Seasonal and regional variation of pan-arctic surface air temperature over the instrumental record, J. Climate, 17, 3263–3282, doi:10.1175/1520-0442(2004)017<3263:SARVOP>2.0.CO;2, 2004. 717

GMDD
8, 715–759, 2015
Improved physical permafrost dynamics in the JULES land surface model
S. Chadburn et al.

Richards, L. A.: Capillary conduction of liquids through porous mediums, J. Appl. Phys., 1, 318–333, 1931. 720
Rinke, A., Kuhry, P., and Dethloff, K.: Importance of a soil organic layer for Arctic climate: a sensitivity study with an Arctic RCM, Geophys. Res. Lett., 35, L13709, doi:10.1029/2008GL034052, 2008. 719
Riseborough, D., Shiklomanov, N., Etzelmüller, B., Gruber, S., and Marchenko, S.: Recent advances in permafrost modelling, Permafrost Periglac., 19, 137–156, doi:10.1002/ppp.615, 2008. 717
Romanovsky, V. E., Drozdov, D. S., Oberman, N. G., Malkova, G. V., Kholodov, A. L., Marchenko, S. S., Moskalenko, N. G., Sergeev, D. O., Ukraintseva, N. G., Abramov, A. A., Gilichinsky, D. A., and Vasiliev, A. A.: Thermal state of permafrost in Russia, Permafrost Periglac., 21, 136–155, doi:10.1002/ppp.683, 2010. 717
Romanovsky, V. E., Smith, S. L., Christiansen, H. H., Shiklomanov, N. I., Streletskiy, D. A., Drozdov, D. S., Oberman, N. G., Kholodov, A. L., and Marchenko, S. S.: Permafrost (Arctic Report Card 2013) available at: http://www.arctic.noaa.gov/reportcard (last access: 27 January 2015), 2013. 717
Schaphoff, S., Heyder, U., Ostberg, S., Gerten, D., Heinke, J., and Lucht, W.: Contribution of permafrost soils to the global carbon budget, Environ. Res. Lett., 8, 014026, doi:10.1088/1748-9326/8/1/014026, 2013. 717
Schneider von Deimling, T., Meinshausen, M., Levermann, A., Huber, V., Frieler, K., Lawrence, D. M., and Brovkin, V.: Estimating the near-surface permafrost-carbon feedback on global warming, Biogeosciences, 9, 649–665, doi:10.5194/bg-9-649-2012, 2012. 717
Soudzilovskaia, N. A., van Bodegom, P. M., and Cornelissen, J. H.: Dominant bryophyte control over high-latitude soil temperature fluctuations predicted by heat transfer traits, field moisture regime and laws of thermal insulation, Funct. Ecol., 27, 1442–1454, doi:10.1111/1365-2435.12127, 2013. 722
Stevens, M. B., Smerdon, J. E., González-Rouco, J. F., Stieglitz, M., and Beltrami, H.: Effects of bottom boundary placement on subsurface heat storage: implications for climate model simulations, Geophys. Res. Lett., 34, L02702, doi:10.1029/2006GL028546, 2007. 719
Stocker, T., Qin, D., Plattner, G.-K., Tignor, M., Allen, S., Boschung, J., Nauels, A., Xia, Y., Bex, V., and Midgley, P. M. (Eds.): Climate Change 2013: The Physical Science Basis. Contribution of Working Group I to the Fifth Assessment Report of the Intergovernmen-

GMDD
8, 715–759, 2015
Improved physical permafrost dynamics in the JULES land surface model
S. Chadburn et al.

tal Panel on Climate Change, IPCC, Cambridge University Press, available at: http://www.climatechange2013.org/ (last access: 27 January 2015), 2013. 717

Sturm, M. and Holmgren, J.: Differences in compaction behavior of three climate classes of snow, Ann. Glaciol., 26, 125–130, 1998. 736

Tarnocai, C., Canadell, J. G., Schuur, E. A. G., Kuhry, P., Mazhitova, G., and Zimov, S.: Soil organic carbon pools in the northern circumpolar permafrost region, Global Biogeochem. Cy., 23, GB2023, doi:10.1029/2008GB003327, 2009. 717

Tian, W., Li, X., Wang, X.-S., and Hu, B. X.: Coupling a groundwater model with a land surface model to improve water and energy cycle simulation, Hydrol. Earth Syst. Sci. Discuss., 9, 1163–1205, doi:10.5194/hessd-9-1163-2012, 2012. 737

Vionnet, V., Brun, E., Morin, S., Boone, A., Faroux, S., Le Moigne, P., Martin, E., and Willemet, J.-M.: The detailed snowpack scheme Crocus and its implementation in SURFEX v7.2, Geosci. Model Dev., 5, 773–791, doi:10.5194/gmd-5-773-2012, 2012. 736

Weedon, G. P.: Readme file for the "WFDEI" dataset, available at: http://www.eu-watch.org/gfx_content/documents/README-WFDEI.pdf (last access: 27 January 2015), 2013. 727

Weedon, G. P., Gomes, S., Viterbo, P., Österle, H., Adam, J. C., Bellouin, N., Boucher, O., and Best., M.: The WATCH forcing data 1958–2001: a meteorological forcing dataset for land surface- and hydrological-models., WATCH technical report, p. 41, available at: http://www.eu-watch.org/publications (last access: 27 January 2015), 2010. 727

Weedon, G. P., Gomes, S., Viterbo, P., Shuttleworth, W. J., Blyth, E., Österle, H., Adam, J. C., Bellouin, N., Boucher, O., and Best, M.: Creation of the WATCH forcing data and its use to assess global and regional reference crop evaporation over land during the twentieth century, J. Hydrometeorol., 12, 823–847, doi:10.1175/2011JHM1369.1, 2011. 727

Westermann, S., Schuler, T. V., Gisnås, K., and Etzelmüller, B.: Transient thermal modeling of permafrost conditions in Southern Norway, The Cryosphere, 7, 719–739, doi:10.5194/tc-7-719-2013, 2013. 719

Westermann, S., Elberling, B., Højlund Pedersen, S., Stendel, M., Hansen, B. U., and Liston, G. E.: Future permafrost conditions along environmental gradients in Zackenberg, Greenland, The Cryosphere Discuss., 8, 3907–3948, doi:10.5194/tcd-8-3907-2014, 2014. 717

Williams, P. and Smith, M.: The Frozen Earth: Fundamentals of Geocryology, Studies in Polar Res., Cambridge University Press, available at: http://books.google.co.uk/books?id=YYCvQAAACAAJ (last access: 27 January 2015), 1991. 722, 723, 725

GMDD
8, 715–759, 2015

Improved physical permafrost dynamics in the JULES land surface model

S. Chadburn et al.

Yi, S., Wischnewski, K., Langer, M., Muster, S., and Boike, J.: Freeze/thaw processes in complex permafrost landscapes of northern Siberia simulated using the TEM ecosystem model: impact of thermokarst ponds and lakes, Geosci. Model Dev., 7, 1671–1689, doi:10.5194/gmd-7-1671-2014, 2014. 726, 737

Zubrzycki, S., Kutzbach, L., Grosse, G., Desyatkin, A., and Pfeiffer, E.-M.: Organic carbon and total nitrogen stocks in soils of the Lena River Delta, PANGAEA, doi:10.1594/PANGAEA.826958, 2013. 728

Table 1. List of JULES simulations carried out. ρ_{fresh} is the density of fresh snow.

Simulation	Layers	Depth	Bedrock	Moss	Organic	New snow	ρ_{fresh}	Moisture
Std	4	3 m	N	N	N	N	130 kg m^{-3}	dynamic
Min14	14	3 m	N	N	N	N	130 kg m^{-3}	dynamic
MinD	28	10 m	50 m	N	N	N	130 kg m^{-3}	dynamic
MinmossD	28	10 m	50 m	Y	N	N	130 kg m^{-3}	dynamic
OrgD	28	10 m	50 m	N	Y	N	130 kg m^{-3}	dynamic
OrgmossD	28	10 m	50 m	Y	Y	N	130 kg m^{-3}	dynamic
OrgmossDS	28	10 m	50 m	Y	Y	Y	130 kg m^{-3}	dynamic
ρ_{fresh} = 170	28	10 m	50 m	Y	Y	Y	170 kg m^{-3}	dynamic
Saturated	28	10 m	50 m	Y	Y	Y	170 kg m^{-3}	fixed

GMDD
8, 715–759, 2015

Improved physical permafrost dynamics in the JULES land surface model

S. Chadburn et al.

Table 2. Simulated and observed soil temperatures on Samoylov Island: annual means and amplitude of annual cycles. The observations (bottom row) give the actual mean temperature (°C) and the simulations give the bias relative to that mean. 9.8 and 18 m observations are from a 27 m borehole. The 0.32 m observations are from a polygon centre. Std simulation values are interpolated to 0.32 m.

	Bias in mean (°C)			Annual cycle (°C)			RMSE
Depth:	0.32 m	9.8 m	18 m	0.32 m	9.8 m	18 m	0.32 m
Year(s):	2004	2007+10	2007+10	2004	2007+10	2007+10	2004
Std	∼ +1.9	–	-	∼ 29	–	–	∼ 4.5
Min14l	+2.2	–	–	30	–	–	4.8
MinD	+1.6	+0.9	+0.4	30	1.0	0.16	5.0
MinmossD	+0.5	0.0	−0.4	26	1.0	0.14	4.0
OrgD	+0.1	−0.4	−0.8	25	0.96	0.15	4.0
OrgmossD	−0.4	−1.0	−1.3	22	0.98	0.12	4.1
OrgmossDS	+0.8	+0.6	+0.4	21	0.82	0.15	3.4
Saturated	*+0.2*	*0.0*	*−0.3*	*26*	*0.94*	*0.20*	*2.7*
Observations	**−9.9**	**−8.6**	**−8.9**	**23**	**1.5**	**0.14**	–

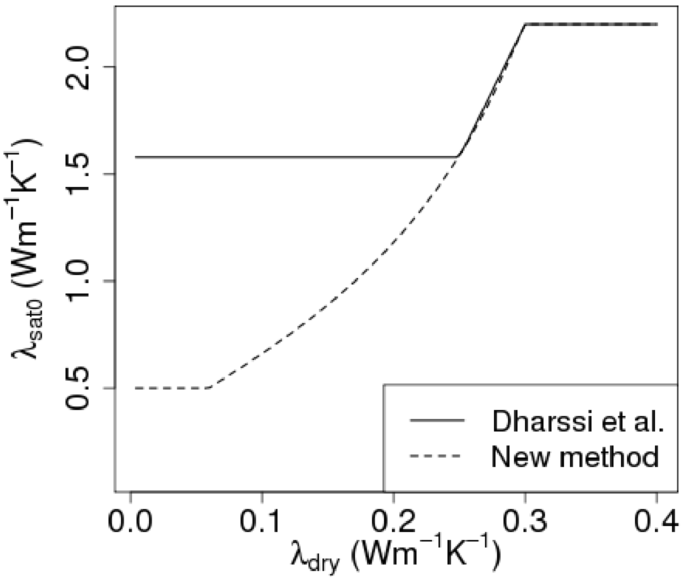

Figure 1. New method of calculating saturated thermal conductivity (λ_{sat0}) from dry thermal conductivity (λ_{dry}), compared with the standard method. See Appendix A, Eq. (A10) for the Dharssi parameterisation, and Appendix A, Eq. (A11) for the new method, which is modified to include organic soils.

GMDD
8, 715–759, 2015

Improved physical permafrost dynamics in the JULES land surface model

S. Chadburn et al.

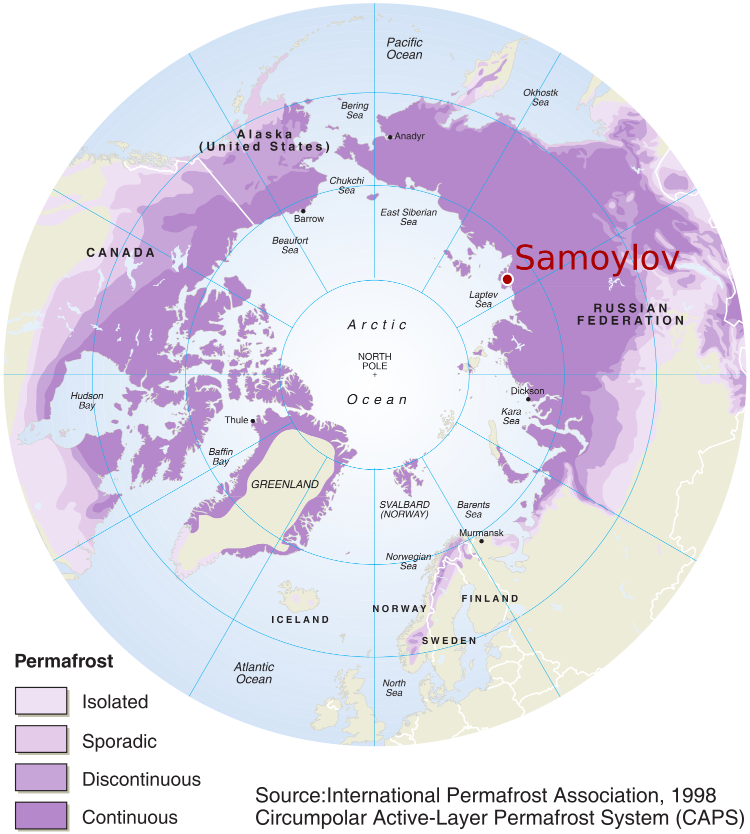

Figure 2. Map showing location of Samoylov Island and Northern Hemisphere permafrost distribution (Brown et al., 1998).

GMDD
8, 715–759, 2015

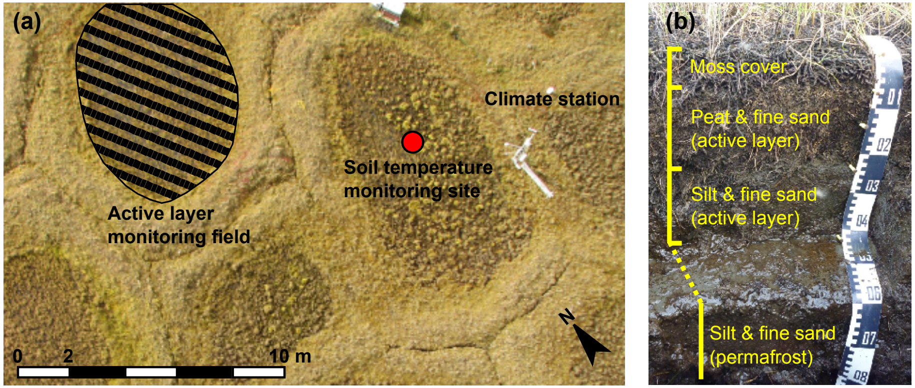

Figure 3. Images from Samoylov Island site. **(a)** Aerial view showing monitoring stations. **(b)** Typical soil profile showing moss layer, organic layer and mineral soil.

GMDD
8, 715–759, 2015

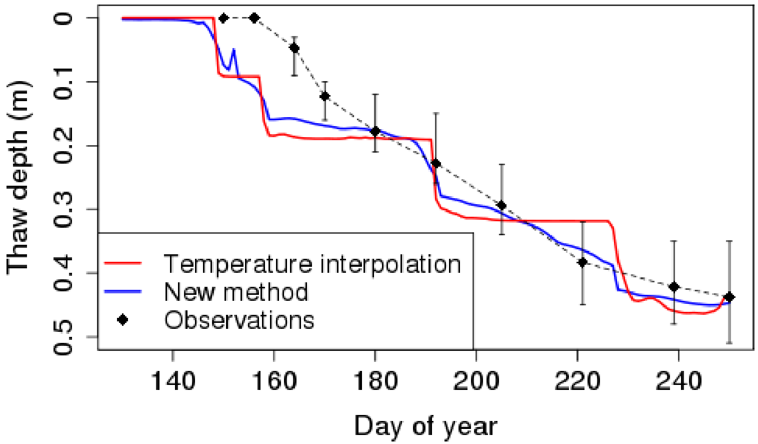

Figure 4. Thaw depth for thawing period in 2006. JULES simulation orgmossDS compared with observations, showing the difference between two methods of calculating thaw depth. The temperature method (red line) is limited by the resolution of the soil layers. Observations are means with error bars showing the full range.

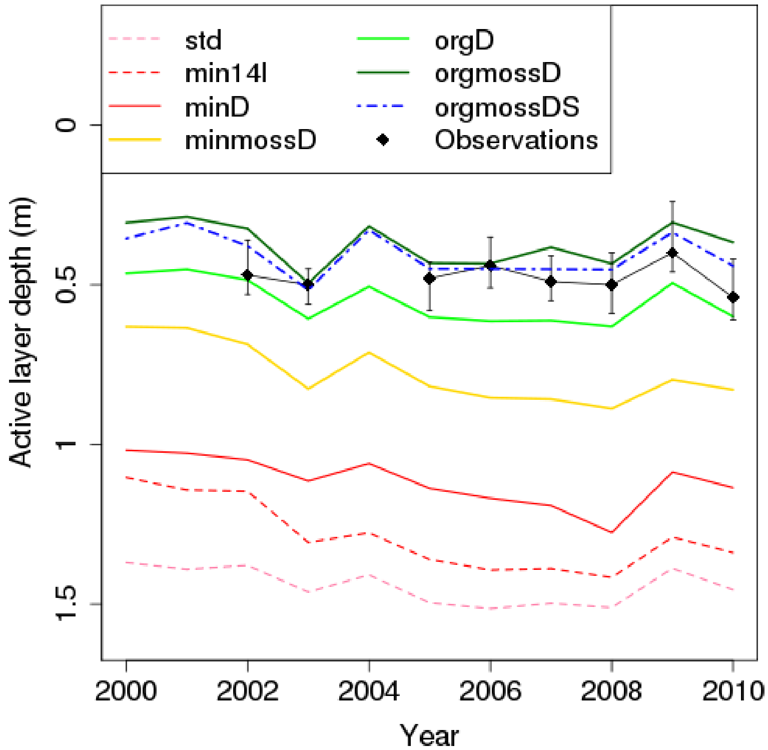

Figure 5. Simulated active layer depth at Samoylov since 2000. Observations show the mean thaw depth from polygon centre active-layer monitoring points (see Fig. 3), with error bars indicating the range of measured values. Simulations begin with the standard 4-layer JULES (std), and improvements are systematically added: higher-resolution soil (min14l), deeper soil (minD), moss cover (minmossD), organic soils (orgD, orgmossD), and the improved snow scheme (orgmossDS).

GMDD
8, 715–759, 2015

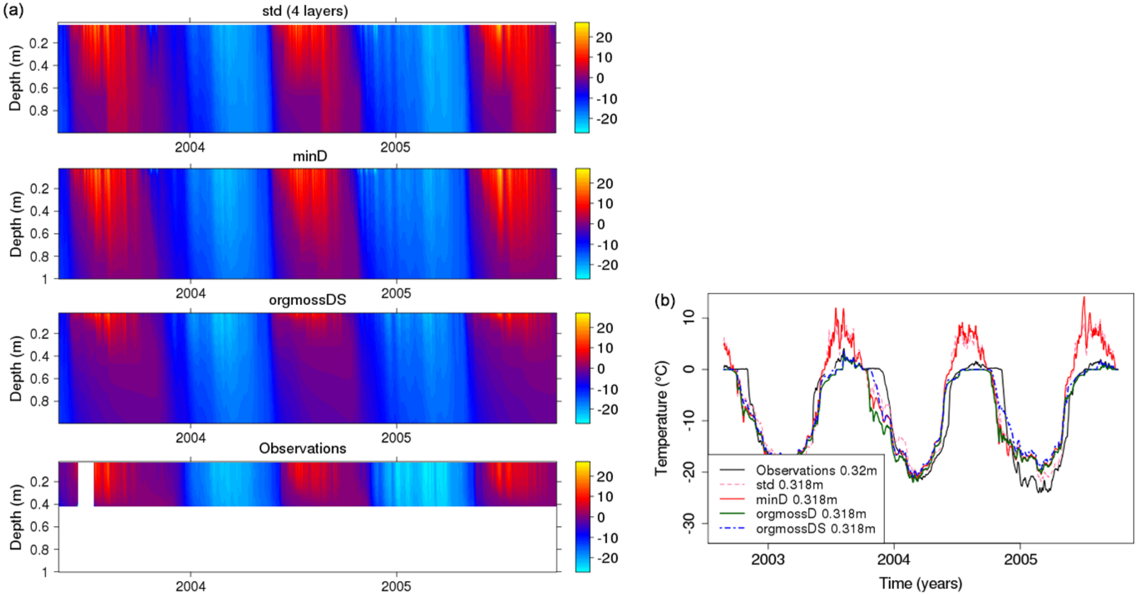

Figure 6. (a) Soil temperatures in active layer, simulated (top 3 plots) and observed (lower plot). The simulations are, from top: standard 4-layer JULES set-up (std); deeper and better-resolved soil (minD); adding to this organic soils, moss, and the improved snow scheme (orgmossDS). Observations are for a polygon centre (see Fig. 3). **(b)** Active layer soil temperatures at 32 cm depth, simulated and observed. The lines represent horizonal slices through the contour plots in Fig. 6a. Additionally, the simulation orgmossD is shown which includes organic soils and moss but not the new snow scheme.

GMDD
8, 715–759, 2015

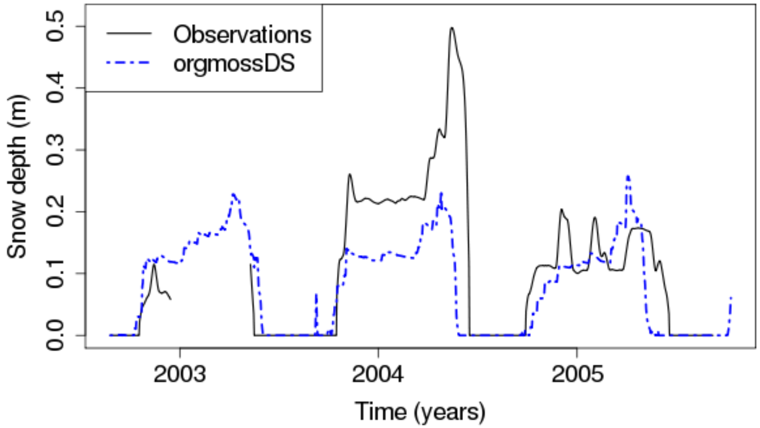

Figure 7. Simulated and observed snow depth at Samoylov over the same years as soil temperatures (Fig. 6b). The simulation orgmossDS includes all model improvements (see Table 1).

GMDD
8, 715–759, 2015

Improved physical permafrost dynamics in the JULES land surface model

S. Chadburn et al.

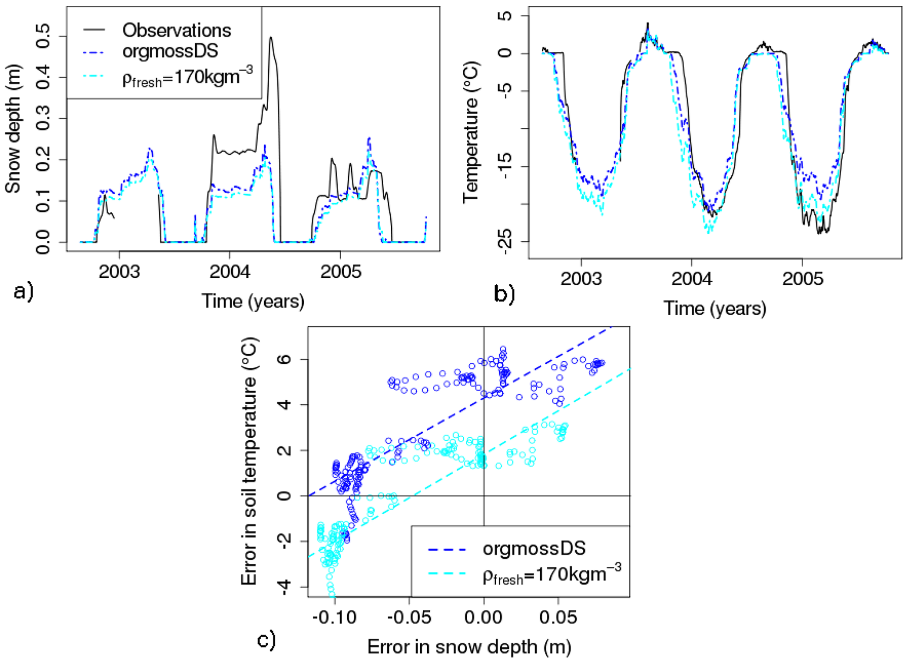

Figure 8. Effect of increasing the fresh snow density (ρ_{fresh}) from 130 to 170 $kg\,m^{-3}$ for the simulation set-up orgmossDS (Table 1). The lower plot compares the error in soil temperatures and snow depths for the coldest months only (January–March) using daily values.

GMDD
8, 715–759, 2015

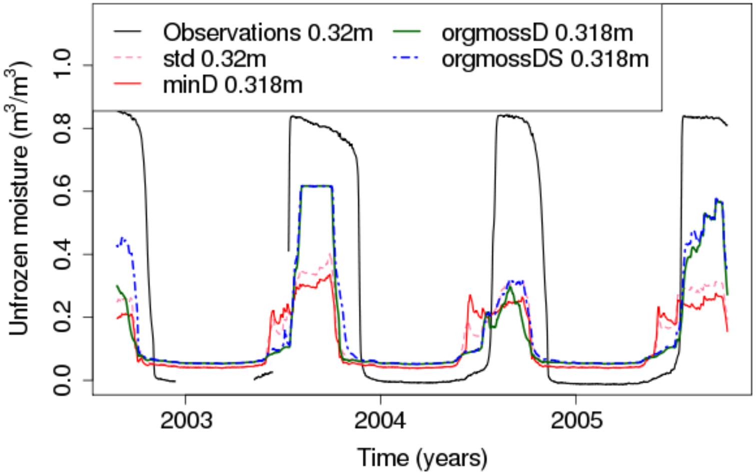

Figure 9. Simulated and observed soil moisture at approximately 32 cm depth. The simulations include the standard JULES set-up (std), and show the effects of a deeper and better-resolved soil (minD), adding organic soils and moss (orgmossD) and improving the snow scheme (orgmossDS). Observations are from a polygon centre.

GMDD
8, 715–759, 2015

Title Page
Abstract | Introduction
Conclusions | References
Tables | Figures
◀| |▶
◀ ▶
Back | Close
Full Screen / Esc
Printer-friendly Version
Interactive Discussion

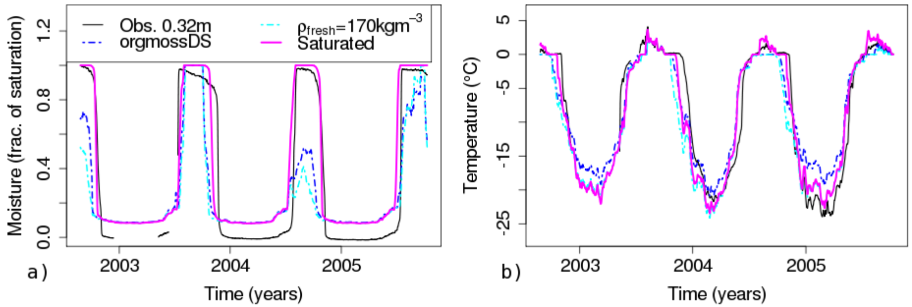

Figure 10. Simulated and observed **(a)** soil moisture and **(b)** temperatures at approximately 32 cm depth. Unfrozen soil moisture is shown as a fraction of saturation. The three simulations show firstly the effect of increasing snow density (compare orgmossDS and $\rho_{\text{fresh}} = 170\,\text{kg}\,\text{m}^{-3}$) and the effect of setting the soil moisture to saturated with increased organic matter (compare $\rho_{\text{fresh}} = 170\,\text{kg}\,\text{m}^{-3}$ and *Saturated*). Observations are from a polygon centre.

GMDD
8, 715–759, 2015

Improved physical permafrost dynamics in the JULES land surface model

S. Chadburn et al.

Title Page
Abstract | Introduction
Conclusions | References
Tables | Figures
◂◂ | ▸▸
◂ | ▸
Back | Close
Full Screen / Esc
Printer-friendly Version
Interactive Discussion